

Influence of compositions of modified blends of polyamide/poly(vinyl alcohol) on the methanol/gasoline fuel barrier properties of polyethylene/modified blends of polyamide/poly(vinyl alcohol) bottles

JEN-TAUT YEH*, LI-HUNG WANG

Graduate School of Fiber and Polymer Engineering, National Taiwan University of Science and Technology, Taipei, Taiwan
E-mail: jyeh@hp730.TX.ntust.edu.tw

KAN-NAN CHEN

Department of Chemistry, Tamkang University, Tamsui, Taiwan

WERN-SHIARNG JOU

Department of Mold and Die Engineering, National Kaohsiung Institute of Technology, Kaohsiung, Taiwan

Polyamide (PA), poly(vinyl alcohol) (PVA) and the blends of PA and PVA were modified by a compatibilizer (CP) to make modified polyamide (MPA), modified PVA (MPVA) and modified PA/PVA (MPAPVA) blends through reactive extrusion. The MPVA and MPA hot-pressed sheets exhibit the best and worst methanol/gasoline fuel permeation resistance among these modified resins, which show much better methanol/gasoline fuel permeation resistance than pure PE resin. It is worth noting that the methanol/gasoline fuel permeation resistance of MPAPVA sheets improves consistently with their PVA contents. Similarly, after blending these barrier resins with PE, the methanol/gasoline fuel permeation resistance of the blended bottles improves to become significantly better than that of pure PE bottles. Further investigations found that the hydrocarbon components with 5 to 10 main-chain carbon atoms present in methanol/gasoline fuels were successfully blocked during the permeation tests. However, the order of barrier improvement of PE/MPA, PE/MPAPVA and PE/MPVA bottles does not completely correspond to the order of the barrier improvement of the base barrier resins before blending and blow-molding with PE. For instance, the PE/MPVA and PE/MPAPVA bottle series with a PVA/PA weight ratio of 4 : 1 exhibit poorer methanol/gasoline fuel permeation resistance than all the other PE/MPAPVA bottles, although the base MPVA and MPAPVA with a 4 : 1 PVA/PA weight ratio are associated with better permeation resistance than the other MPAPVA resins prepared in this study. These interesting phenomena were investigated in terms of the melt shear viscosities, chemical structure and morphology of the barrier resins present in their corresponding bottles.

© 2001 Kluwer Academic Publishers

1. Introduction

In the last decade, people have been looking for new fuels to replace gasoline because the petroleum will soon be depleted later this century. The methanol/gasoline fuel has been proved to be one of the best replacements for gasoline because of its low cost, high efficiency, and low air pollution. Polyolefins, such as high-density polyethylene (HDPE), have been considered as a potential material for storing methanol/gasoline fuels instead of metal because methanol may cause metal corrosion.

Moreover, HDPE has been widely used as industrial and household containers for storage of various fluids because of its lightweight, easy design and processing, recyclability, low cost, safety, high chemical corrosive resistance, and flexibility. However, HDPE is notorious for its poor permeation resistance to hydrocarbon solvents, such as gasoline, because the escaped solvents may result in serious environmental pollution.

The gasoline molecules penetration through the HDPE container follows the solution-diffusion

* To whom all correspondence should be addressed.

mechanism through the homogeneous amorphous phase of the material. Permeant molecules dissolve into the inner surface of HDPE, diffuse through the amorphous region, reach outer surface, and evaporate into the environment. Several technologies have been developed to reduce the solubility or diffusivity of the hydrocarbon solvents, and hence, improve the permeation resistance of HDPE. These methods include surface treatment of PE by fluorination or sulfonation [1,2], multi-layer co-extrusion of PE, compatibilizer precursor (CP) and polyamide (PA) [1, 2], laminar-blend blow molding of PE, CP and PA blends [3–5] or laminar-blend blow molding of PE and modified polyamide (MPA) [6–14]. Among these developed techniques, the “laminar-blend-blow-molding process” that forms a layered structure containing numerous discontinuous overlapping platelets of barrier resins such as PA or MPA in a PE matrix is one of the well proven methods to enhance the resistance of HDPE containers against hydrocarbon permeation [3–14]. The heterogeneous laminar blends exhibit significantly better hydrocarbon permeation resistance than the conventional homogeneous blends associated with uniform dispersed PA within the PE matrix [6–18]. However, the barrier properties of the lamellar structure formed by modified polyamide or polyamide/compatibilizer blends are not good enough to prevent the permeation of methanol/gasoline fuels. In contrast, poly(vinyl alcohol) (PVA) has been reported [13,18] that can further improve the barrier resistance of PE or PE/MPA containers against methanol/gasoline fuel permeation. In our previous investigation [13], PA and PVA resins were modified by a CP to make various compositions of modified polyamide (MPA) and modified PA/PVA (MPAPVA) blends through reactive extrusion. Good methanol/gasoline fuel permeation resistance together with clearly defined MPAPVA and MPA laminar structures were found in containers blow-molded from PE/MPAPVA and PE/MPA blends, respectively. The permeation resistance of PE/MPAPVA bottles against methanol/gasoline fuels is even better than that of PE/MPA bottles of the same CP content. On the other hand, the best barrier resistance of PE/MPAPVA and PE/MPA bottles against methanol/gasoline fuels was obtained as the CP content contained in MPAPVA and MPA reached an optimum value of about 20 wt% [13]. However, it is not completely clear what are the optimum compositions for obtaining the best permeation resistance of the plastic containers against methanol/gasoline fuel, and what are the underlying mechanisms accounting for these interesting phenomena.

Following our previous investigation [13], the main purpose of this study is to further justify the optimum composition of MPAPVA for obtaining enhanced permeation resistance of PE/MPAPVA bottles, and to investigate the underlying mechanisms accounting for the above improved barrier properties. In order to understand the permeation mechanisms of methanol/gasoline fuels, the weight loss together with the compositions of methanol/gasoline fuels before and after the per-

meation tests were determined. The barrier properties of PE, PE/MPA, PE/MPVA and PE/MPAPVA with different PVA contents were investigated in this study.

2. Experimental

2.1. Materials and sample preparation

The commercial grade polyamide (PA) and poly(vinyl alcohol) (PVA) resins were modified by a compatibilizer precursor (CP) to make modified polyamide (MPA), modified poly(vinyl alcohol) (MPVA), and modified blends of polyamide/poly(vinyl alcohol) (MPAPVA) through reactive extrusion. The compatibilizer precursor used in this study is a zinc-neutralized ethylene/acrylic acid copolymer. The polyamide (PA) used is nylon 6, which was obtained from Formosa Chemicals and Fiber Corporation with a trade name of Sunylon 6N. The polyethylene (Taisox 9003), PVA (BF-05) and antioxidant (Irganox B225) were purchased from Formosa Plastic, Chang Chun Petrochemical and Ciba-Geigy Corporation, respectively.

Before melt blending, PA and PVA were dried at 80°C for 16 hrs, and CP was dried at 60°C for 8 hrs, respectively. About 1500 ppm of antioxidant were first dry-blended with the dried components of PA/CP, PVA/CP or PA/PVA/CP, and then fed into a twin screw extruder to prepare MPA, MPVA or MPAPVA resins, respectively. The compositions of MPA, MPVA and MPAPVA resins prepared in this study are summarized in Table I.

The PA, PVA, MPA, MPVA and MPAPVA resins prepared above were then dried at 80°C for 16 hrs, and then dry-blended with PE at a weight ratio of 90 : 10 before blow-molding. The mixed PE/MPA, PE/MPVA and PE/MPAPVA blends were then blow-molded at an extrusion temperature of 230°C and a screw speed of 15 rpm. The blow-molded bottles weigh about 50 g with a volume capacity of 500 ml and a wall thickness of about 1 mm.

TABLE I Compositions of MPA, MPVA and MPAPVA resins

Samples	PA (wt%)	PVA (wt%)	CP (wt%)
MPA ₁₀	90.0	—	10.0
MPA ₂ PVA ₁₋₁₀	60.0	30.0	10.0
MPA ₁ PVA ₁₋₁₀	45.0	45.0	10.0
MPA ₁ PVA ₂₋₁₀	30.0	60.0	10.0
MPA ₁ PVA ₄₋₁₀	18.0	72.0	10.0
MPVA ₁₀	—	90.0	10.0
MPA ₂₀	80.0	—	20.0
MPA ₂ PVA ₁₋₂₀	53.3	26.7	20.0
MPA ₁ PVA ₁₋₂₀	40.0	40.0	20.0
MPA ₁ PVA ₂₋₂₀	26.7	53.3	20.0
MPA ₁ PVA ₄₋₂₀	16.0	64.0	20.0
MPVA ₂₀	—	80.0	20.0
MPA ₃₀	70.0	—	30.0
MPA ₂ PVA ₁₋₃₀	46.7	23.3	30.0
MPA ₁ PVA ₁₋₃₀	35.0	35.0	30.0
MPA ₁ PVA ₂₋₃₀	23.3	46.7	30.0
MPA ₁ PVA ₄₋₃₀	14.0	56.0	30.0
MPVA ₃₀	—	70.0	30.0

2.2. Permeation resistance of bottles and hot-pressed sheets

The permeation resistance of the blow-molded bottles against methanol/gasoline fuels was evaluated by measuring the weight loss of methanol/gasoline fuels filled in the bottles. The PE, PE/MPA, PE/MPVA and PE/MPAPVA bottles were initially filled with 300 g of various compositions of methanol/gasoline fuels with the mixing ratios of 0/100, 20/80, 40/60, 60/40, 80/20 and 100/0, respectively. The weight losses of methanol/gasoline fuels were monitored after 14 days at a storage temperature of 40°C. On the other hand, the permeation resistance of PA, MPA, MPAPVA and MPVA against methanol/gasoline fuels was determined based on their hot-pressed sheets, because PA, MPA, MPAPVA and MPVA resins are difficult to blow-mold due to their poor melt strengths. The dried pellets of PA, MPA, MPAPVA and MPVA were hot-pressed at 230°C into sheets about 1 mm thick and then cut into circles of a diameter of 140 mm. For purposes of comparison, similar hot-pressed sheets were also prepared from base PE resin using the same compression-molding machine, while operated at a compression temperature of 170°C. The circular PE, PA, MPA, MPAPVA and MPVA sheets were sealed as lids on the top of test flasks filled with 300 g of methanol/gasoline fuels. However, the permeation resistance of the hot-pressed PVA sheet was not determined because it is too brittle to be sealed as lids on the top of test flasks filled with methanol/gasoline fuels. The permeation barrier properties of these circular sheets were then determined by measuring the weight losses of methanol/gasoline fuels after holding the flasks at 40°C for 14 days.

2.3. Compositions of residual methanol/gasoline fuels

The composition of methanol/gasoline fuels before and after permeation tests were determined using a China 8900 Gas Chromatography (GC) equipped with a hydrogen flame ionization detector. A Restek Alumina Plot capillary column was used for separation of the methanol/gasoline fuels. The capillary column has an inside diameter of 0.53 mm and a length of 30 m. The methanol/gasoline fuels before and after permeation tests were injected into the GC at 230°C to determine their compositions. Helium (He) flowing at $20 \times 10^{-6} \text{ m}^3/\text{min}$ was used as the carrier gas at 220°C. In order to improve the separation efficiency, the capillary column was raised from 30 to 210°C at a heating rate of 4°C/min, and the detector temperature was set at 230°C. The main components contained in unleaded gasoline are non-polar linear, cyclic and aromatic hydrocarbons (about 5 to 10 carbons) and some polar liquid, such as alcohol, ether and other additives [19–21]. Table II summarized the retention time of the main components of methanol/gasoline fuel containing 20 wt% methanol (M20) detected by GC. Similar results were found on the methanol/gasoline fuels with methanol contents other than 20 wt%. For purposes of comparison and convenience, the residual

TABLE II The retention time of the main components of M20 methanol/gasoline fuels detected by GC

Retention Time (Min.)	Components	Formulas
1.91	<i>n</i> -Pentane	C ₅ H ₁₂
4.24	<i>n</i> -Hexane	C ₆ H ₁₄
4.77	Benzene	C ₆ H ₆
5.37	Methanol	CH ₄ O
6.05	<i>n</i> -Heptane	C ₇ H ₁₆
7.51	Toluence	C ₇ H ₈
9.81	<i>n</i> -Decane	C ₁₀ H ₂₂
9.87	<i>n</i> -Octane	C ₈ H ₁₈
14.92	Xylene	C ₈ H ₁₀
20.62	Ethanol	C ₂ H ₆ O
23.48	<i>i</i> -Propanol	C ₃ H ₈ O
23.51	Decalin	C ₁₀ H ₁₈
32.20	DMF	C ₃ H ₇ ON

weight percentage of the hydrocarbon components with 5 to 10 main-chain carbon atoms (i.e. *n*-pentane, xylene, toluene, decalin) and methanol of the M20 methanol/gasoline fuel were selected and determined by GC to illustrate the compositions of the residual methanol/gasoline fuels after permeation tests. The residual wt% of each solvent was determined by the area ratio of each solvent peak after permeation test to that before permeation test.

2.4. Rheological and morphology properties

The melt shear viscosities (η_s) of PE, PA, PVA, MPA, MPVA and MPAPVA resins were measured at 230°C and at shear rates ranging from 30 up to 120 s⁻¹ using a Rosand Precision Advanced Capillary Extrusion Rheometer equipped with a capillary of 1 mm diameter. In order to observe the deformation structures of MPA, MPVA, and MPAPVA in PE/MPA, PE/MPVA, and PE/MPAPVA bottles, respectively, these blow-molded bottles were fractured in liquid nitrogen and etched with formic acid. The etched samples were then gold-coated and examined using a Jeol JSM-5200 Scanning Electron Microscope (SEM).

3. Results and discussion

3.1. Rheological properties

The melt shear viscosities (η_s) of PE, PA, PVA, MPA, MPVA and MPAPVA resins are summarized in Figs 1 to 3. It is worth noting that PE exhibits the highest η_s , while PVA shows the lowest η_s among these base resins at various melt shear rates. Moreover, the η_s of the modified PA and PVA (i.e. MPA and MPVA) are significantly higher than those of their corresponding base PA and PVA resins, and increase consistently with the CP contents contained in MPA and MPVA resins, respectively. However, it is worth noting that η_s of MPAPVA resins are much lower than those of corresponding MPA resins with the same CP content (see Figs 1 to 3). In fact, at a fixed CP content, η_s of MPAPVA resins decrease consistently as their PVA contents increase, and MPVA resins exhibit even lower

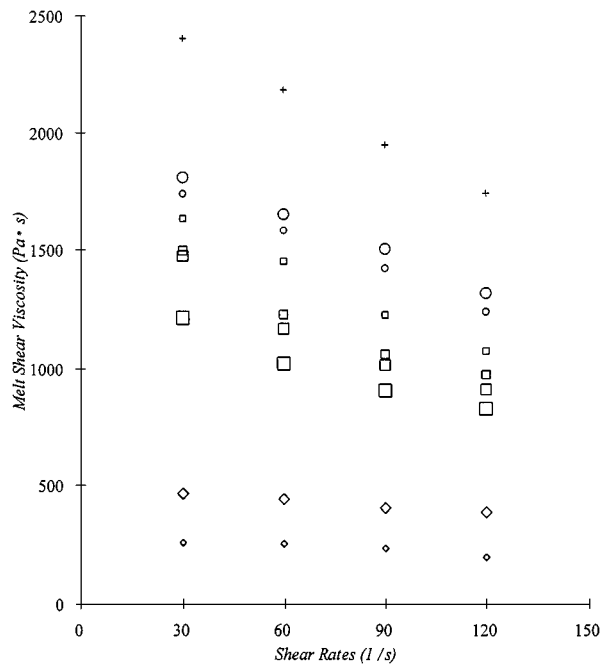


Figure 1 Melt shear viscosities of PE (+), PA (○), PVA (◇), MPA₁₀ (○), MPA₂PVA₁₋₁₀ (◻), MPA₁PVA₁₋₁₀ (◻), MPA₁PVA₂₋₁₀ (◻), MPA₁PVA₄₋₁₀ (◻) and MPVA₁₀ (◇) resins measured at 230°C and various shear rates.

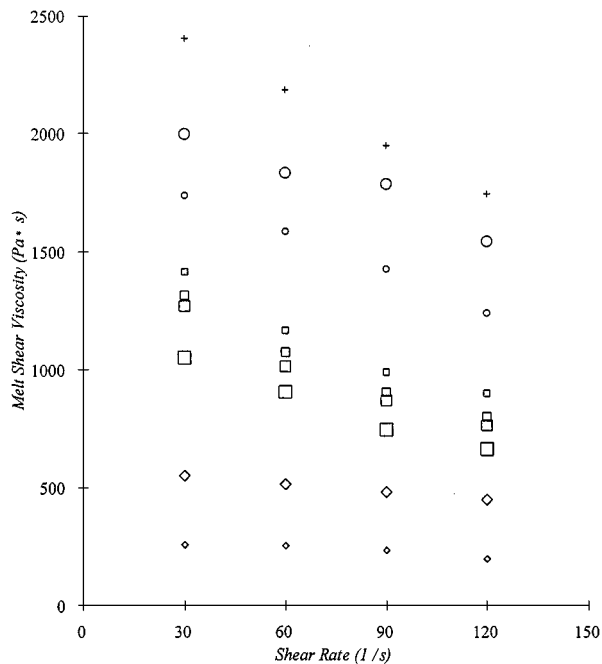


Figure 3 Melt shear viscosities of PE (+), PA (○), PVA (◇), MPA₃₀ (○), MPA₂PVA₁₋₃₀ (◻), MPA₁PVA₁₋₃₀ (◻), MPA₁PVA₂₋₃₀ (◻), MPA₁PVA₄₋₃₀ (◻) and MPVA₃₀ (◇) resins measured at 230°C and various shear rates.

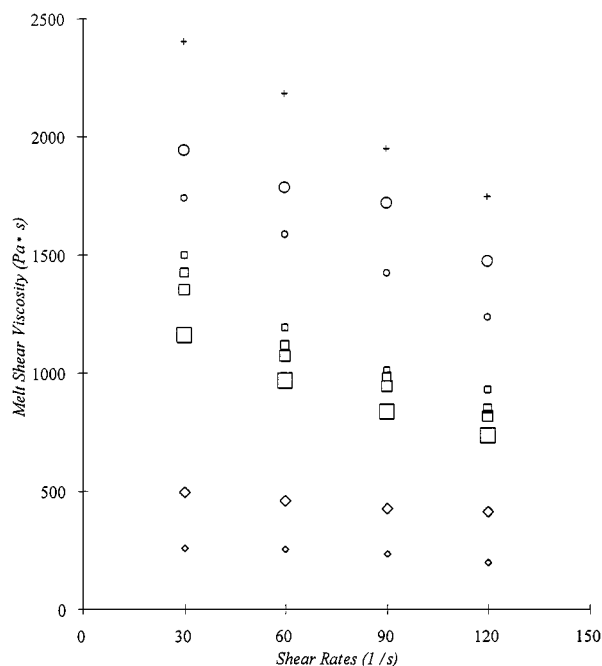


Figure 2 Melt shear viscosities of PE (+), PA (○), PVA (◇), MPA₂₀ (○), MPA₂PVA₁₋₂₀ (◻), MPA₁PVA₁₋₂₀ (◻), MPA₁PVA₂₋₂₀ (◻), MPA₁PVA₄₋₂₀ (◻), and MPVA₂₀ (◇) resins measured at 230°C and various shear rates.

η_s than all the MPAPVA resins with the same CP contents. Presumably, the reaction of carboxyl groups of CP with the terminal amine groups of PA and hydroxyl groups of PVA can generate larger “crosslinked” CP/PA and CP/PVA copolymer molecules and make their η_s higher than those of their genetic PA and PVA resins, respectively. Similarly, the carboxyl groups of CP can react with both of the terminal amine and

hydroxyl groups at the same time during the reactive extrusion process of MPAPVA resins. However, the melt shear viscosity of PVA is significantly lower than that of PA resin used in this study. Based on these premises, the majority of the “crosslinked” copolymers could be relatively small and/or short CP/PVA or CP/PVA/PA rather than large and long CP/PA copolymers, as the PVA contents contained in MPAPVA increase. Therefore, the η_s of MPAPVA resins prepared in this study decrease consistently with increasing PVA contents and are all lower (higher) than those of corresponding MPA (MPVA) resins with the same CP contents.

3.2. Morphology of PE/MPA, PE/MPAPVA and PE/MPVA bottles

Typical fracture surfaces of PE/MPA, PE/MPAPVA and PE/MPVA bottles are shown in Figs 4 to 6. Many clearly defined MPA laminas were found distributed in PE matrices through the wall thickness direction of the PE/MPA bottles (see Figs 4a, 5a and 6a). Similar to those found in PE/MPA bottles, many clearly defined MPAPVA laminas were found on the fracture surfaces of PE/MPA₂PVA₁₋₁₀, PE/MPA₂PVA₁₋₂₀ and PE/MPA₂PVA₁₋₃₀ bottles (see Figs 4b, 5b and 6b). However, the MPAPVA laminas become less demarcated as their η_s decrease. As shown in Figs 4 to 6, some MPAPVA laminas found on the fracture surfaces of PE/MPAPVA bottles are not elongated, continuous but broken and obscure laminas, wherein their η_s are significantly lower than those of their corresponding MPA₂PVA₁₋₁₀, MPA₂PVA₁₋₂₀ and MPA₂PVA₁₋₃₀ resins, respectively. Moreover, it is interesting to note that almost only broken, discontinuous MPVA laminas

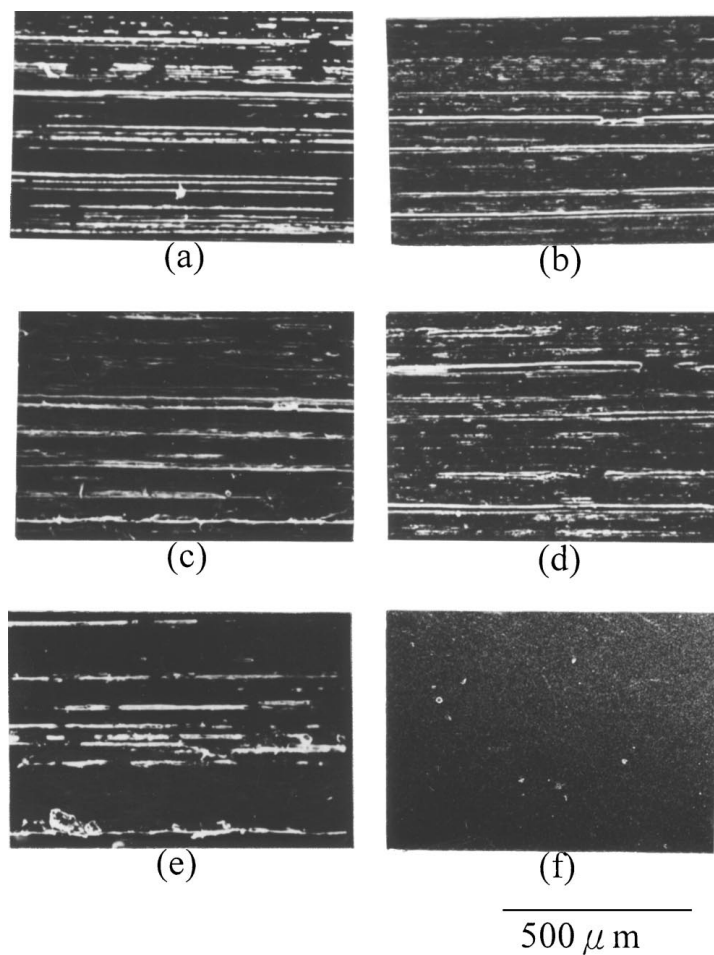


Figure 4 Morphologies of (a) PE/MPA₁₀, (b) PE/MPA₂PVA₁₋₁₀, (c) PE/MPA₁PVA₁₋₁₀, (d) PE/MPA₁PVA₂₋₁₀, (e) PE/MPA₁PVA₄₋₁₀ and (f) PE/MPVA₁₀ bottles.

were found on the fracture surfaces of PE/MPVA bottles, wherein MPVA resins exhibit significantly lower η_s than all the MPAPVA resins with the same CP content (see Figs 4f, 5f and 6f). As mentioned previously, PE exhibits a higher melt shear viscosity than any of the other base and/or modified barrier resins (i.e. MPA, MPVA and MPAPVA). Presumably, the barrier resins are well adhered to PE and can be biaxially stretched by the PE matrix into demarcated laminar structures as long as they are associated with an optimum melt shear viscosity ratio to PE [12], wherein the barrier melts are strong enough but not too hard to be stretched during the blow-molding process of PE/MPA, PE/MPVA and PE/MPAPVA blends. Therefore, many demarcated and elongated MPA laminas were found on the fracture surfaces of PE/MPA bottles. In contrast, the melt shear viscosities and strength of MPAPVA resins are lower than those of corresponding MPA resins and reduce consistently with the PVA contents contained in MPAPVA resins. As a consequence, these MPAPVA resins with relatively low melt strength were stretched by PE melt into somewhat broken and less demarcated MPAPVA laminas during the blow-molding process of PE/MPAPVA bottles. Moreover, the MPVA resins with the lowest η_s and melt strength were stretched into many broken laminas during the blow-molding processes of PE/MPVA bottles.

3.3. Barrier properties of hot-pressed PE, PA, PVA, MPA, MPVA and MPAPVA sheets

The methanol/gasoline fuel permeation rates of PE, PA, MPA, MPVA and MPAPVA sheets are summarized in Figs 7 to 9. As expected, PE sheets exhibit the worst resistance against methanol/gasoline fuel permeation among these base resins. In contrast, PA and the modified barrier resins (i.e. MPA, MPVA and MPAPVA) sheets exhibit much better methanol/gasoline fuel permeation resistance than PE sheets. It is interesting to note that all MPA and MPVA resins exhibit better permeation resistance than the base PA resin without CP modification, respectively. In fact, the methanol/gasoline fuel permeation resistance of MPVA resins is always better than that of MPA resins with the same CP content. In contrast, the MPAPVA sheets exhibit significantly better barrier properties against methanol/gasoline fuel permeation than the corresponding MPA sheets with the same CP content. It is further interesting to note that the permeation resistance of MPAPVA sheets improves consistently as their PVA contents increase. As shown in Figs 7 to 9, MPVA₁₀, MPVA₂₀ and MPVA₃₀ sheets exhibit the slowest, but MPA₂PVA₁₋₁₀, MPA₂PVA₁₋₂₀ and MPA₂PVA₁₋₃₀ sheets exhibit the fastest permeation rate against methanol/gasoline fuels among the

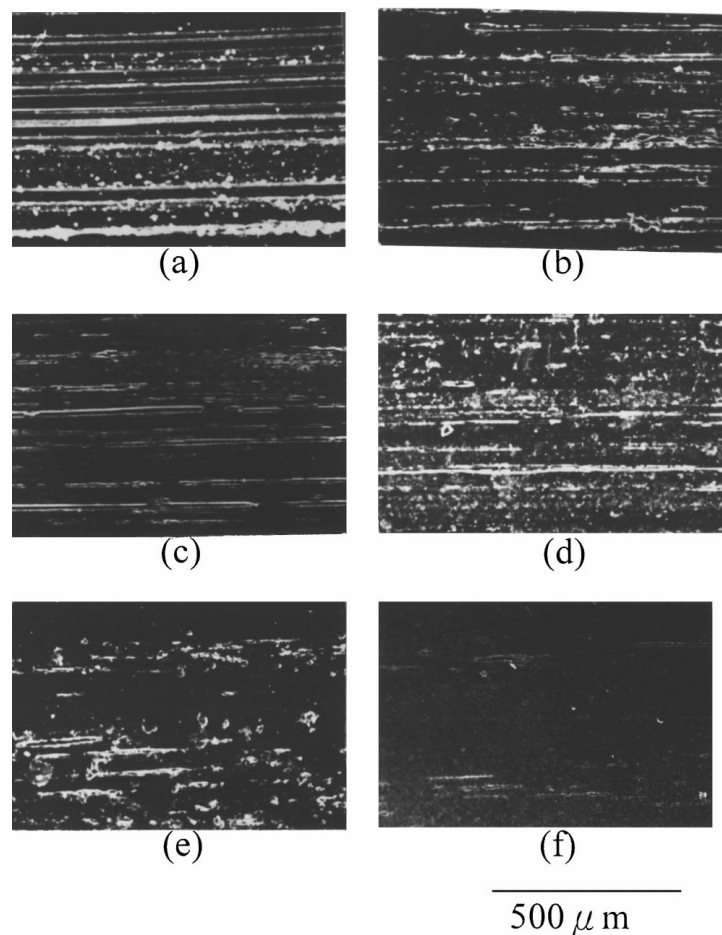


Figure 5 Morphologies of (a) PE/MPA₂₀, (b) PE/MPA₂PVA₁₋₂₀, (c) PE/MPA₁PVA₁₋₂₀, (d) PE/MPA₁PVA₂₋₂₀, (e) PE/MPA₁PVA₄₋₂₀ and (f) PE/MPVA₂₀ bottles.

MPA_xPVA_{y-20}, MPA_xPVA_{y-20} and MPA_xPVA_{y-30} sheet series, respectively. These results clearly suggest that the PVA content has a beneficial influence on the methanol/gasoline fuel permeation resistance of the MPAPVA resins.

3.4. Barrier properties of PE, PE/MPA, PE/MPVA and PE/MPAPVA bottles

The methanol/gasoline fuel permeation rates of PE, PE/MPA, PE/MPVA and PE/MPAPVA bottles are summarized in Figs 10 to 12. The base PE bottles exhibited slightly better resistance against methanol permeation than PE/MPA, PE/MPVA and PE/MPAPVA bottles. However, the methanol/gasoline fuel permeation rates of PE bottles increase significantly after adding certain amounts of gasoline in methanol. The typical compositions of methanol/gasoline fuels before and after permeation tests of PE, PE/MPA, PE/MPVA and PE/MPAPVA bottles are summarized in Figs 13 to 17. Significant amounts of hydrocarbon components with 5 to 10 main-chain carbon atoms (i.e. *n*-pentane, xylene, toluene, decalin) present in M20 methanol/gasoline fuels permeated through PE bottles, while the relatively polar methanol component remained almost intact without permeation after 14 days at 40°C. In contrast, after blending the barrier resins into the PE matrix, the methanol/gasoline fuel

permeation rates of the PE/MPA, PE/MPVA and PE/MPAPVA bottles were significantly reduced compared to those of pure PE bottles. Further investigations indicate that these hydrocarbon components present in methanol/gasoline fuels were significantly blocked during the permeation tests of these blended PE/MPA, PE/MPVA and PE/MPAPVA bottles (see Figs 13 to 16). In contrast, the permeated amounts of methanol of these PE/MPA, PE/MPVA and PE/MPAPVA bottles are about the same as those of pure PE bottles after permeation tests (see Fig. 17). On the other hand, it is interesting to note that the order of barrier improvement of these blended bottles does not completely correspond to the order of the barrier improvement of the base barrier resins before blending with PE (see Figs 7 to 12). For instance, the methanol/gasoline permeation rates of PE/MPAPVA bottles reduce consistently as the PVA contents of MPAPVA resins increase from 0 to about 60 wt% (i.e. MPA₁PVA₂₋₁₀, MPA₁PVA₂₋₂₀ and MPA₁PVA₂₋₃₀ samples). However, after this value, the barrier improvements of PE/MPAPVA bottles against methanol/gasoline permeation decrease consistently as the PVA contents increase. As shown in Figs 10 to 12, PE/MPA₁PVA₄₋₁₀, PE/MPA₁PVA₄₋₂₀ and PE/MPA₁PVA₄₋₃₀ bottles exhibit significantly faster permeation rates than PE/MPA₁PVA₂₋₁₀, PE/MPA₁PVA₂₋₂₀ and PE/MPA₁PVA₂₋₃₀ bottles, respectively. Moreover, PE/MPVA₁₀, PE/MPVA₂₀ and

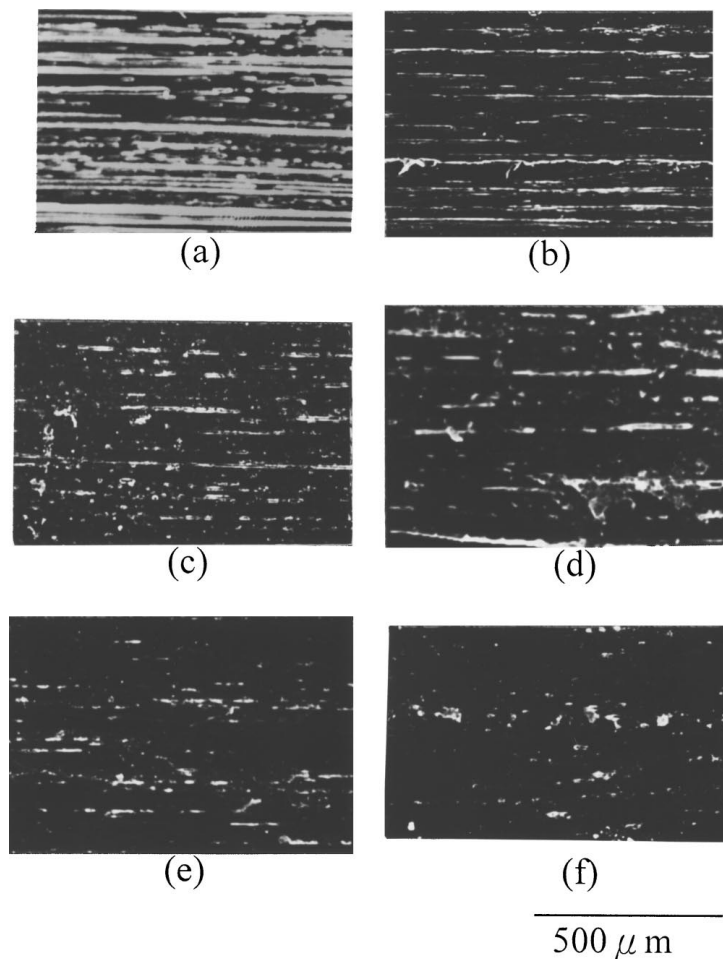


Figure 6 Morphologies of (a) PE/MPA₃₀, (b) PE/MPA₂PVA₁₋₃₀, (c) PE/MPA₁PVA₁₋₃₀, (d) PE/MPA₁PVA₂₋₃₀, (e) PE/MPA₁PVA₄₋₃₀ and (f) PE/MPVA₃₀ bottles.

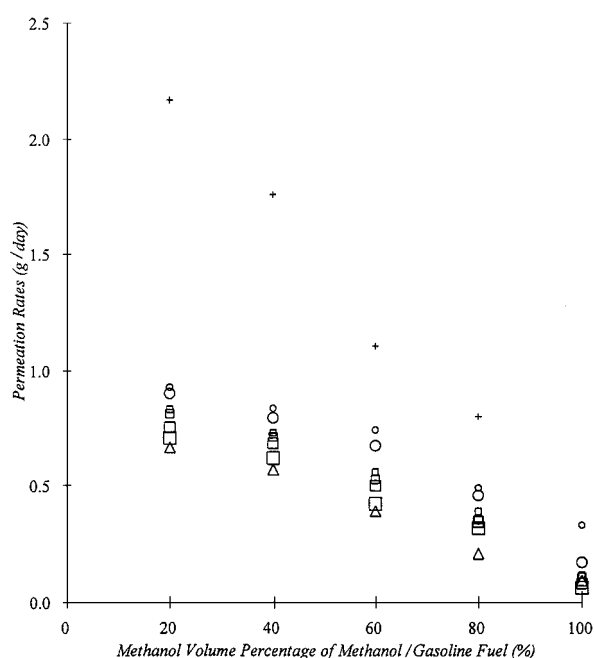


Figure 7 Methanol/gasoline fuel permeation rates of PE (+), PA (○), MPA₁₀ (○), MPVA₁₀, (△), MPA₂PVA₁₋₁₀ (◐), MPA₁PVA₁₋₁₀ (◑), MPA₁PVA₂₋₁₀ (◒), and MPA₁PVA₄₋₁₀ (◓) sheets.

PE/MPVA₃₀ exhibit ever faster permeation rates than the corresponding PE/MPAPVA bottle series, although the base MPVA resins are associated with significantly better methanol/gasoline permeation resistance than

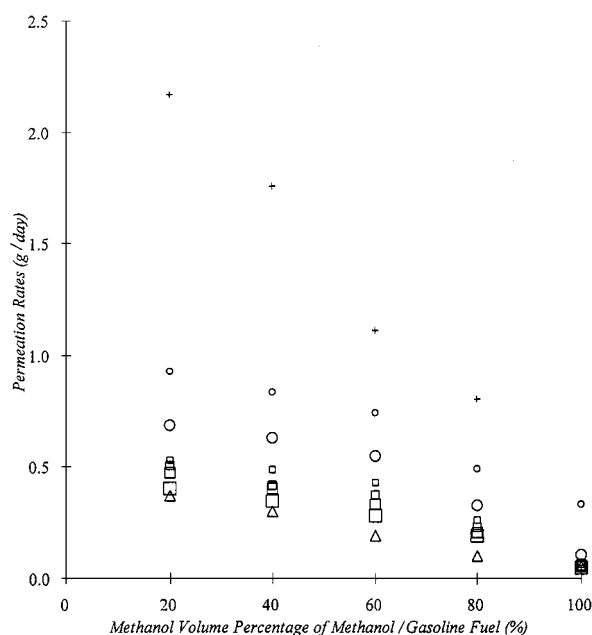


Figure 8 Methanol/gasoline fuel permeation rates of PE (+), PA (○), MPA₂₀ (○), MPVA₂₀ (△), MPA₂PVA₁₋₂₀ (◐), MPA₁PVA₁₋₂₀ (◑), MPA₁PVA₂₋₂₀ (◒), and MPA₁PVA₄₋₂₀ (◓) sheets.

their corresponding base MPAPVA resins before blending and blow-molding with PE. It is not completely clear what accounts for these interesting behaviors. Presumably, the level of barrier improvements of PE/MPA,

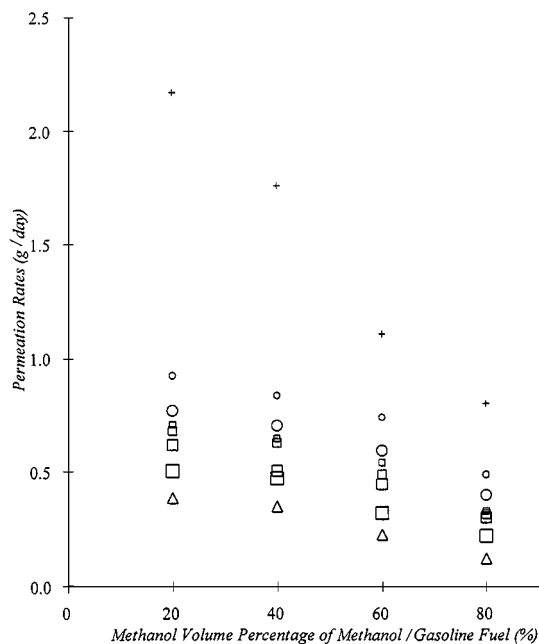


Figure 9 Methanol/gasoline fuel permeation rates of PE (+), PA (○), MPA₃₀ (◐), MPVA₃₀ (△), MPA₂PVA₁₋₃₀ (◑), MPA₁PVA₁₋₃₀ (◒), MPA₁PVA₂₋₃₀ (◓), and MPA₁PVA₄₋₃₀ (◔) sheets.

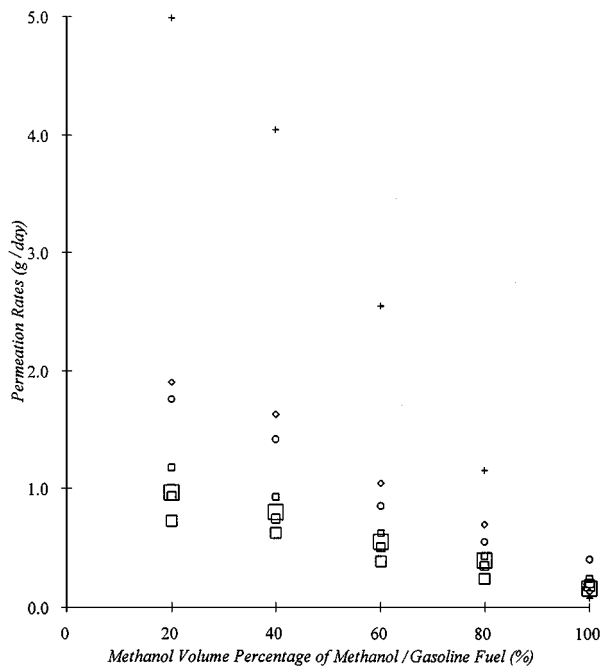


Figure 11 Methanol/gasoline fuel permeation rates of PE (+), PE/MPA₂₀ (○), PE/MPVA₂₀ (◊), PE/MPA₂PVA₁₋₂₀ (◑), PE/MPA₁PVA₁₋₂₀ (◒), PE/MPA₁PVA₂₋₂₀ (◓), and PE/MPA₁PVA₄₋₂₀ (◔) bottles.

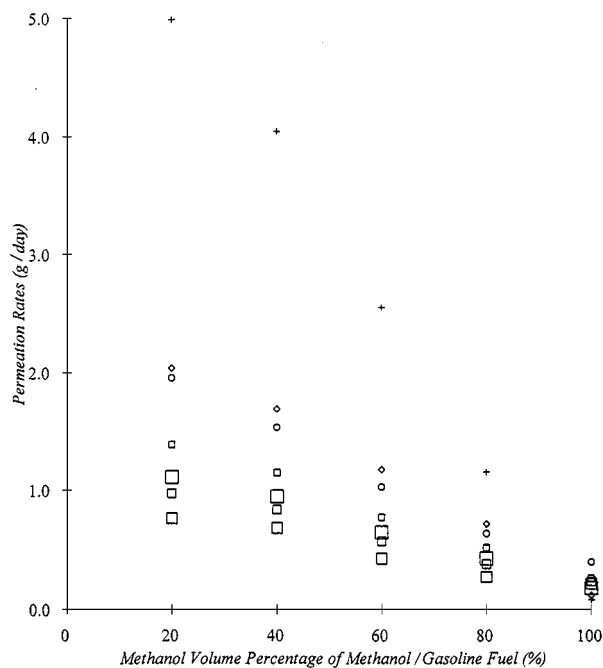


Figure 10 Methanol/gasoline fuel permeation rates of PE (+), PE/MPA₁₀ (○), PE/MPVA₁₀ (◊), PE/MPA₂PVA₁₋₁₀ (◑), PE/MPA₁PVA₁₋₁₀ (◒), PE/MPA₁PVA₂₋₁₀ (◓), and PE/MPA₁PVA₄₋₁₀ (◔) bottles.

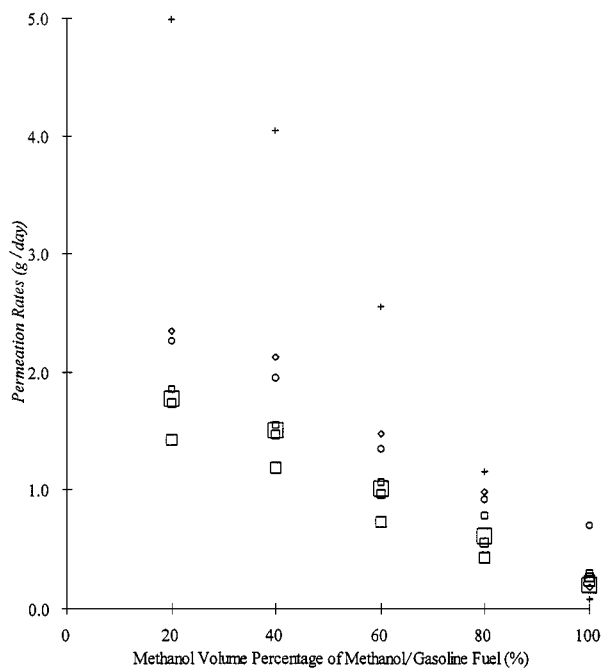


Figure 12 Methanol/gasoline fuel permeation rates of PE (+), PE/MPA₃₀ (○), PE/MPVA₃₀ (◊), PE/MPA₂PVA₁₋₃₀ (◑), PE/MPA₁PVA₁₋₃₀ (◒), PE/MPA₁PVA₂₋₃₀ (◓), and PE/MPA₁PVA₄₋₃₀ (◔) bottles.

PE/MPAPVA and PE/MPVA blends depends significantly on the barrier properties of the base barrier resins. Moreover, the demarcated and elongated MPA, MPAPVA and MPVA laminas can further improve the permeation resistance of PE/MPA, PE/MPAPVA and PE/MPVA bottles against methanol/gasoline fuels, respectively, since the elongated laminar structures

can prolong the permeation period of the non-polar hydrocarbon molecules through the bottles further than those of bottles of relatively obscure and broken laminar structures. As observed in the previous section, the MPAPVA laminas found in PE/MPAPVA bottles become less demarcated and somewhat broken as the PVA contents of MPAPVA resins

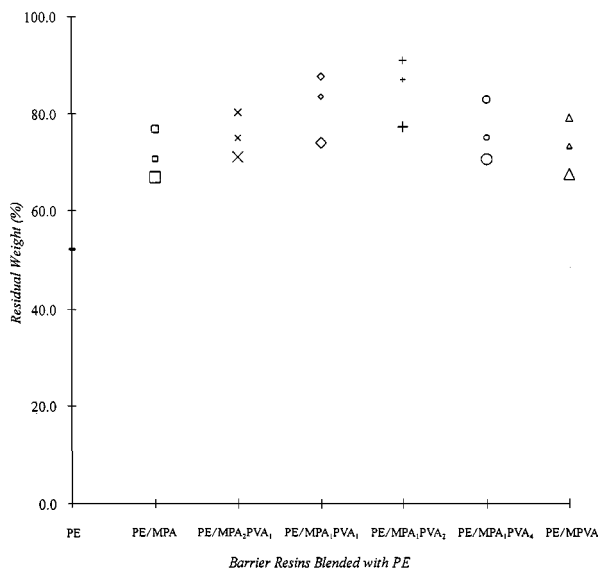


Figure 13 The *n*-pentane residual weight (%) of M20 methanol/gasoline fuel after permeation test in PE (-), PE/MPA₁₀ (×), PE/MPA₂PVA₁₋₁₀ (◻), PE/MPA₁PVA₁₋₁₀ (◊), PE/MPA₁PVA₂₋₁₀ (+), PE/MPA₁PVA₄₋₁₀ (○), PE/MPVA₁₀ (Δ), PE/MPA₂₀ (×), PE/MPA₂PVA₁₋₂₀ (◻), PE/MPA₁PVA₁₋₂₀ (◊), PE/MPA₁PVA₂₋₂₀ (+), PE/MPA₁PVA₄₋₂₀ (○), PE/MPVA₂₀ (Δ), PE/MPA₃₀ (×), PE/MPA₂PVA₁₋₃₀ (◻), PE/MPA₁PVA₁₋₃₀ (◊), PE/MPA₁PVA₂₋₃₀ (+), PE/MPA₁PVA₄₋₃₀ (○) and PE/MPVA₃₀ (Δ).

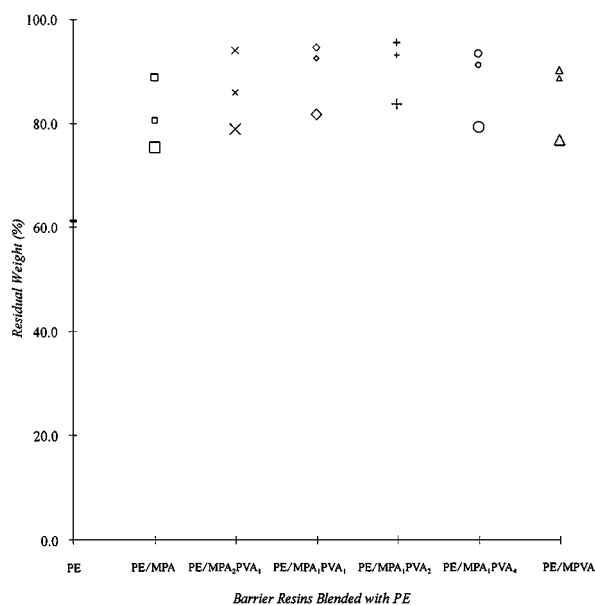


Figure 14 The xylene residual weight (%) of M20 methanol/gasoline fuel after permeation test in PE (-), PE/MPA₁₀ (×), PE/MPA₂PVA₁₋₁₀ (◻), PE/MPA₁PVA₁₋₁₀ (◊), PE/MPA₁PVA₂₋₁₀ (+), PE/MPA₁PVA₄₋₁₀ (○), PE/MPVA₁₀ (Δ), PE/MPA₂₀ (×), PE/MPA₂PVA₁₋₂₀ (◻), PE/MPA₁PVA₁₋₂₀ (◊), PE/MPA₁PVA₂₋₂₀ (+), PE/MPA₁PVA₄₋₂₀ (○), PE/MPVA₂₀ (Δ), PE/MPA₃₀ (×), PE/MPA₂PVA₁₋₃₀ (◻), PE/MPA₁PVA₁₋₃₀ (◊), PE/MPA₁PVA₂₋₃₀ (+), PE/MPA₁PVA₄₋₃₀ (○) and PE/MPVA₃₀ (Δ).

increase. In fact, almost only broken and discontinuous MPVA laminar structures were found on the fracture surfaces of PE/MPVA bottles. The decreasing permeation resistance of PE/MPAPVA and PE/MPVA bottles with increasing PVA contents is, therefore, attributed to the broken and less demarcated

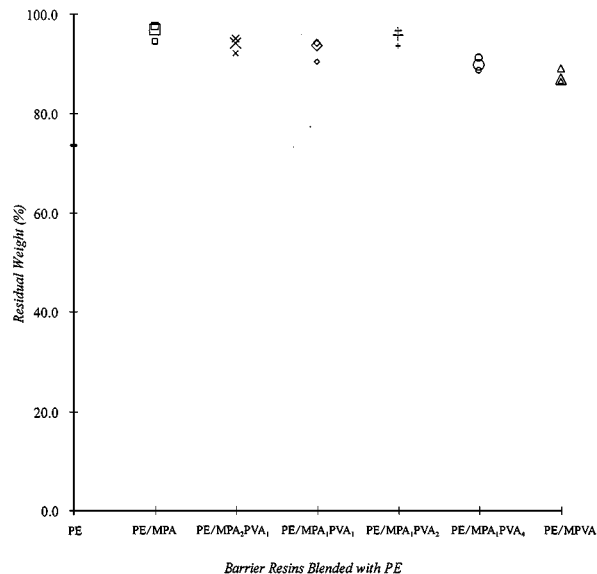


Figure 15 The toluene residual weight (%) of M20 methanol/gasoline fuel after permeation test in PE (-), PE/MPA₁₀ (×), PE/MPA₂PVA₁₋₁₀ (◻), PE/MPA₁PVA₁₋₁₀ (◊), PE/MPA₁PVA₂₋₁₀ (+), PE/MPA₁PVA₄₋₁₀ (○), PE/MPVA₁₀ (Δ), PE/MPA₂₀ (×), PE/MPA₂PVA₁₋₂₀ (◻), PE/MPA₁PVA₁₋₂₀ (◊), PE/MPA₁PVA₂₋₂₀ (+), PE/MPA₁PVA₄₋₂₀ (○), PE/MPVA₂₀ (Δ), PE/MPA₃₀ (×), PE/MPA₂PVA₁₋₃₀ (◻), PE/MPA₁PVA₁₋₃₀ (◊), PE/MPA₁PVA₂₋₃₀ (+), PE/MPA₁PVA₄₋₃₀ (○) and PE/MPVA₃₀ (Δ).

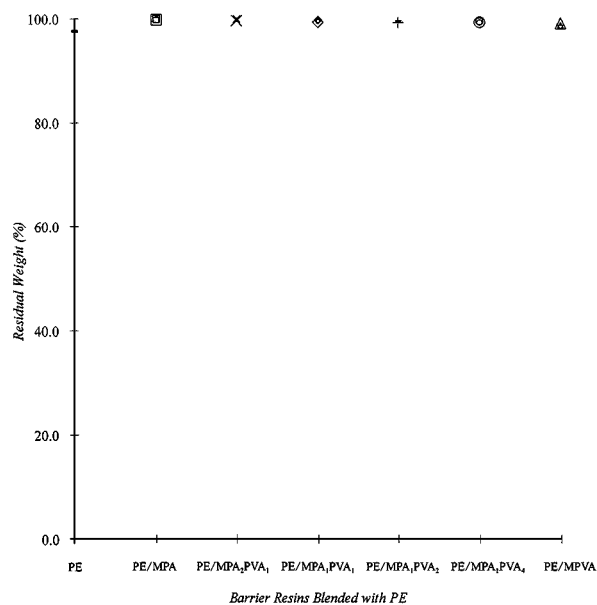


Figure 16 The decalin residual weight (%) of M20 methanol/gasoline fuel after permeation test in PE (-), PE/MPA₁₀ (×), PE/MPA₂PVA₁₋₁₀ (◻), PE/MPA₁PVA₁₋₁₀ (◊), PE/MPA₁PVA₂₋₁₀ (+), PE/MPA₁PVA₄₋₁₀ (○), PE/MPVA₁₀ (Δ), PE/MPA₂₀ (×), PE/MPA₂PVA₁₋₂₀ (◻), PE/MPA₁PVA₁₋₂₀ (◊), PE/MPA₁PVA₂₋₂₀ (+), PE/MPA₁PVA₄₋₂₀ (○), PE/MPVA₂₀ (Δ), PE/MPA₃₀ (×), PE/MPA₂PVA₁₋₃₀ (◻), PE/MPA₁PVA₁₋₃₀ (◊), PE/MPA₁PVA₂₋₃₀ (+), PE/MPA₁PVA₄₋₃₀ (○) and PE/MPVA₃₀ (Δ).

MPAPVA and MPVA laminas present in their corresponding bottles, although the base MPA₁PVA_{4-X} resins exhibit significant better methanol/gasoline fuel permeation resistance than the corresponding MPA or other MPAPVA resins with the same CP contents.

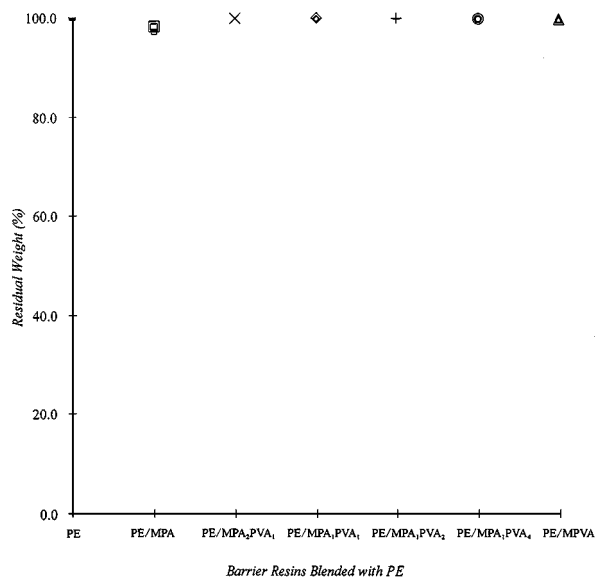


Figure 17 The methanol residual weight (%) of M20 methanol/gasoline fuel after permeation test in PE (-), PE/MPA₁₀ (×), PE/MPA₂PVA₁₋₁₀ (□), PE/MPA₁PVA₁₋₁₀ (◇), PE/MPA₁PVA₂₋₁₀ (+), PE/MPA₁PVA₄₋₁₀ (○), PE/MPVA₁₀ (△), PE/MPA₂₀ (×), PE/MPA₂PVA₁₋₂₀ (□), PE/MPA₁PVA₁₋₂₀ (◇), PE/MPA₁PVA₂₋₂₀ (+), PE/MPA₁PVA₄₋₂₀ (○), PE/MPVA₂₀ (△), PE/MPA₃₀ (×), PE/MPA₂PVA₁₋₃₀ (□), PE/MPA₁PVA₁₋₃₀ (◇), PE/MPA₁PVA₂₋₃₀ (+), PE/MPA₁PVA₄₋₃₀ (○) and PE/MPVA₃₀ (△).

4. Conclusion

The hot-pressed sheets of PA and their modified resins (i.e. MPA, MPVA and MPAPVA) exhibit much better methanol/gasoline fuel permeation resistance than the PE sheet, and MPA and MPVA resins exhibit significantly better methanol/gasoline fuel permeation resistance than the base PA resin without CP modification. The MPVA resins exhibit the best, while MPA resins with the same CP contents exhibit the worst resistance against methanol/gasoline fuel permeation among these modified barrier resins. Moreover, the methanol/gasoline permeation resistance of MPAPVA sheets improves consistently as their PVA contents increase. Significant amounts of hydrocarbon components present in methanol/gasoline fuels permeated through PE bottles, while the relatively polar methanol component remained almost intact without permeation after 14 days at 40 °C. In contrast, after blending the barrier resins in PE matrix, most of the hydrocarbon components present in methanol/gasoline fuels were significantly blocked and, hence, the permeation rates of PE/MPA, PE/MPVA and PE/MPAPVA bottles were significantly reduced compared to those of pure PE bottles. On the other hand, it is worth noting that the order of barrier improvement of these blended bottles

does not completely correspond to the order of the barrier improvement of the base barrier resins before blending with PE, as the PVA contents contained in MPAPVA and/or MPVA resins increase to a critical value. The PE/MPA₁PVA_{4-X} and MPVA_X show even poorer permeation resistance than other corresponding PE/MPAPVA bottles although the permeation resistance properties of PE/MPA₁PVA_{4-X} and MPVA_X are better than those of other MPAPVA resins before blow-molding with PE. Further morphological investigations suggest that this decreasing permeation resistance of PE/MPAPVA and/or PE/MPVA bottles is attributed to the broken and less demarcated MPAPVA and/or MPVA laminas present in their corresponding bottles, although the base MPA₁PVA_{4-X} and MPVA_X resins are associated with better methanol/gasoline fuel permeation resistance than MPA or MPAPVA resins with the same CP contents.

References

1. J. H. SCHUT, *Plastics Technol.* **5** (1992) 52.
2. K. CHANDRAMOUL and S. A. JABARIN, *Adv. Polym. Technol.* **14** (1995) 35.
3. P. M. SUBRAMANIAN, U.S. Patent no. 4410482 (1983).
4. *Idem.*, U.S. Patent no. 4444817 (1984).
5. ROBERT LEAVERSUCH, in proceedings of Modern Plastics International, July 24 (McGraw-Hill, Lausanne, Switzerland, 1986).
6. J. T. YEH, C. C. FAN-CHIANG and M. F. CHO, *Polym. Bull.* **35** (1995) 371.
7. J. T. YEH and C. C. FAN-CHIANG, *J. Polym. Res.* **3** (1996) 211.
8. J. T. YEH, C. C. FAN-CHIANG and S. S. YANG, *J. Appl. Polym. Sci.* **8** (1997) 1531.
9. J. T. YEH and C. C. FAN-CHIANG, *ibid.* **66** (1997) 2517.
10. J. T. YEH, C. F. JYAN and S. CHOU, *SPE ANTEC Tech. Papers* **44** (1998) 3567.
11. J. T. YEH and C. F. JYAN, *Polym. Eng. Sci.* **38** (1998) 1482.
12. J. T. YEH, C. F. JYAN, S. S. YANG and S. CHOU, *ibid.* **39** (1999) 1952.
13. J. T. YEH, W. S. JOU and Y. S. SU, *J. Appl. Polym. Sci.* **9** (1999) 2158.
14. J. T. YEH, C. C. CHAO and C. H. CHEN, *ibid.* accepted.
15. P. M. SUBRAMANIAN, *Polym. Eng. Sci.* **25** (1985) 483.
16. *Idem.*, *ibid.* **27** (1987) 663.
17. *Idem.*, in Conference Proceedings—Technical Association of Pulp and Paper Industry; Laminations and coating conference (1984) 341.
18. P. M. SUBRAMANIAN and V. MEHRA, *SPE ANTEC Tech. Papers* **32** (1986) 301.
19. E. R. FANICK, L. R. SMITH, J. A. RUSSELL, W. E. LIKOS and M. AHUJA, SAE Paper 902156 (1990).
20. R. L. FUREY and K. L. PERRY, SAE Paper 912425 (1991).
21. R. D. SCHWARTZ, R. G. MATHEWS and D. J. BRASSEAU, *J. Gas Chromatography* (1967) 257.

Received 4 April

and accepted 17 October 2000